INFLUENCE OF TRIPPING ON SPATIOTEMPORAL CORRELATION BETWEEN VELOCITY AND WALL PRESSURE IN A TURBULENT BOUNDARY LAYER

Yasuyuki Sendai
Department of mechanical systems engineering
Shinshu University
4-17-1 Wakasato, Nagano, Japan
10ta131d@shinshu-u.ac.jp

Masaharu Matsubara
Department of mechanical systems engineering
Shinshu University
4-17-1 Wakasato, Nagano, Japan
mmatsu@shinshu-u.ac.jp

ABSTRACT

The aim of this study is to investigate tripping influence on not only basic statistics such as mean velocity and fluctuation profiles, but also spatiotemporal correlation between the wall pressure and the streamwise velocity fluctuations. In wall-bounded turbulent shear flows, measurements of instantaneous flow fields at the near wall position are restricted by the exists of the wall, though the turbulence production mainly occurs there. The wall pressure and its distribution were focused as an obtainable quantity including rich information related to the turbulence production. Measurements are performed in a flat plate turbulent boundary layer using a hot wire and a spanwise array of 32 MEMS microphone sensors mounted on the wall. The comparison was performed at the same Reynolds number based on the momentum thickness of the boundary layer. The cross-correlation between the streamwise velocity and the wall pressure fluctuations are not affected by the alteration of the tripping devices. On the other hand, its invariable distribution suggests the cross-correlation can be utilized for detecting structure of disturbance in turbulent shear flows.

INTRODUCTION

Recent extensive comparison of numerical results for a turbulent boundary layer indicated considerable discrepancies in both peak fluctuation values and the outer layer profiles(Schlatter and Örlü, 2010). One possibility to explain this inconsistency is dependence of upstream disturbance condition that strictly governs boundary layer transition. It cannot be denied that the transition process affects turbulent flow even further downstream from the transition point. It is known well that a mean velocity profile of the zero-pressure-gradient turbulent boundary layer follows the logarithmic law independent of tripping condition. This does not mean that the profile of the inner layer is invariable because the profile normalized by the quantities derivative of the wall skin friction that is determined by the profile itself. Change of velocity fluctuations normalized by the wall unit are also restricted since the wall-normal Reynolds stress, which is a mean value of production of two velocity fluctuation, strongly relates to the mean velocity profile. For judgement on the tripping effect, comparison of other quantities that are independent of or weakly correlative with the logarithmic law parameters is needed. In this present experiment it is aimed to reveal effect of the tripping on characteristic of the zero-pressure-gradient turbulent boundary layer with focusing autocorrelation of the wall pressure fluctuation and cross-correlation between that and the streamwise velocity fluctuation.

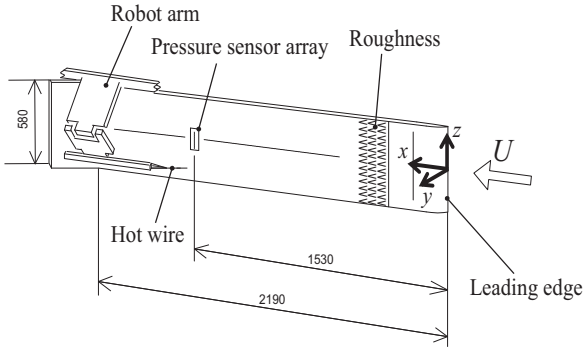

Figure 1. Experimental Setup.

EXPERIMENTAL-SETUP

Experimental setup is shown in Figure 1. The experiment was made in a closed wind tunnel, which had a test sec-

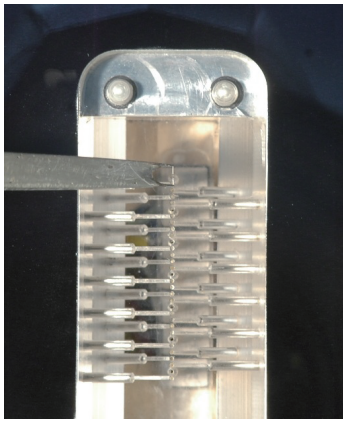

Figure 2. Pressure sensor array and a hot wire probe.

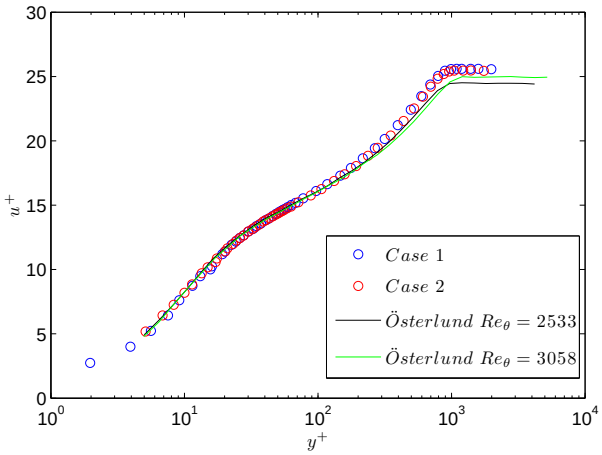

Figure 3. The streamwise mean velocity profiles.

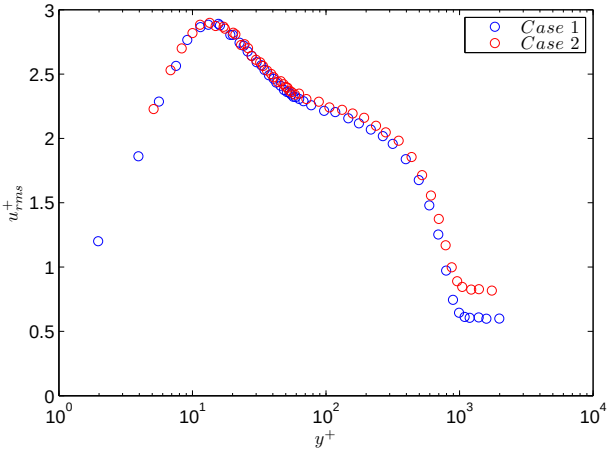

Figure 4. Distributions of the streamwise velocity fluctuation u_{rms}.

tion of a 400 mm width, a 600 mm height and a 4 m length. An aluminum test plate of a 2.1 m length, a 580 mm width and a 10 mm thickness was mounted vertically in the test section with a 100 mm separation from one side wall of the test section. Its leading edge was located at 1510 mm from the exit of a contraction. The other side wall faced to the test surface and a trailing-edge flap were carefully adjusted to prevent separation around the leading edge and to obtain constant streamwise distribution of pressure in the free stream. The coordinate system is denoted by the streamwise, wall-normal and spanwise distances x, y and z from the origin at the center of the leading edge, respectively. Figure 2 shows a hot wire probe above a plug of the pressure sensor array. The pressure sensor array had 32 holes of a 0.5 mm diameter with a spanwise space of 0.8 mm. Each hole was connected to a MEMS microphone. For velocity measurement, the hot wire of 0.5 mm length and 2.5 μm diameter was used. The sensor array and the hot wire were located at $x = 1530$ mm.

Two tripping sets were tested. One set labeled 'Case 1' consists five rows of plastic tapes embossed with letter 'V's located between $x = 315$ and 415 mm. The other set of 'Case 2' had seven rows of the 'V' plastic tapes placed between $x = 150$ and 400 mm. The streamwise spacing of the tapes were regular in each case. For case 2, in addition to the tapes, a strip of No. 100 grit sandpaper was fixed downstream of the plastic tapes. The free stream velocity U_f is 16.9 m/s in Case 1 and 14.6 m/s in Case 2. The free stream velocity U_f was adjusted so that the Reynolds numbers based on the momentum thickness Re_θ at the streamwise position of the sensor array were same in both cases. The momentum thickness θ is 2.69 mm and 3.11 mm, Re_θ is 2841 and 2842, the wall friction velocity u_τ is 0.6610 m/s and 0.5747 m/s in Case 1 and 2, respectively.

RESULTS

The velocity profiles at the streamwise position of the pressure sensor are shown in Figure 3. u_τ was estimated to fit to the universal profile proposed by Chauhan et. al.(2007). The profiles in Cases 1 and 2 are collapsed well and the free stream velocities in the wall unit, U_f/u_τ, are 25.6 and 25.4, respectively. Comparing with the profiles at similar Re_θ measured by Österlund(1999), the present profiles begin to diverge from the logarithmic slope slightly closer to the wall. It is should be noticed that the present profiles in the real scale is different because of the adjusted free velocity about 14 % lower in Case 2.

Distributions of the streamwise velocity fluctuation u_{rms} are shown in Figure 4. The high values of u_{rms} in the free stream are caused by electrical noise from the frequency inverter of the blower. In the inner layer the u_{rms} profiles, including the peak values, are in good agreement, while it is lower in the outer layer in Case 2. This disagreement seems to be from the electrical noise that alters with the represent parameters for the normalization even its value is constant in the dimensional scale.

Contour maps of space-time autocorrelation of the wall pressure in Case 1 and 2 are shown in Figure 5 and 6. The both temporal and spacial scales are normalized in the wall unit as $\Delta z^+ = \Delta z u_\tau/\nu$ and $\Delta t^+ = \Delta t u_\tau U_f/\nu$. Δz and Δt are

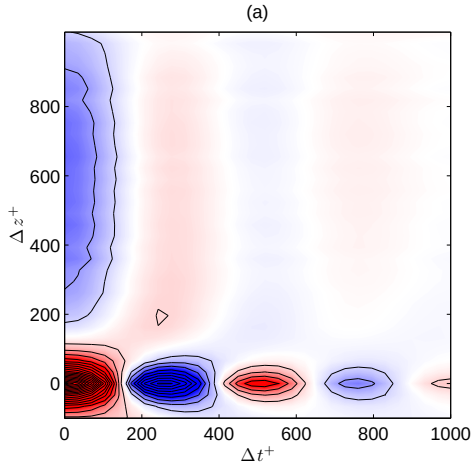

Figure 5. Contour maps of space-time autocorrelation of the wall pressure fluctuation in Case 1. Contour spacing is 5 % and positive and negative regions are colored in red and blue, respectively.

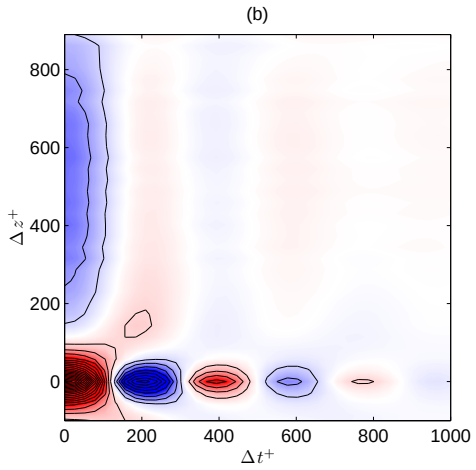

Figure 6. Contour maps of space-time autocorrelation of the wall pressure fluctuation in Case 2. Contour spacing and colorizing are same in. Figure 5.

the spanwise and temporal separation of measurement points. In both cases, two kinds of negative peak appear. One is due to the spanwise structures and others are temporal. In the spanwise distribution at $\Delta t^+ = 0$ the widely spreading negative region is observed. The temporal distributions have constant-spacing positive and negative peaks that indicate periodical pressure fluctuation. The correlation distributions in both cases are basically similar except that the temporal spacing of the peaks is longer in Case 1. The fact that the spacing in the real scale is about 0.7 ms for both case suggests these correlation peaks are due to a resonance of the microphone devices that may have Helmholtz or air column resonances. Fortunately the pressure-velocity correlation has longer scale

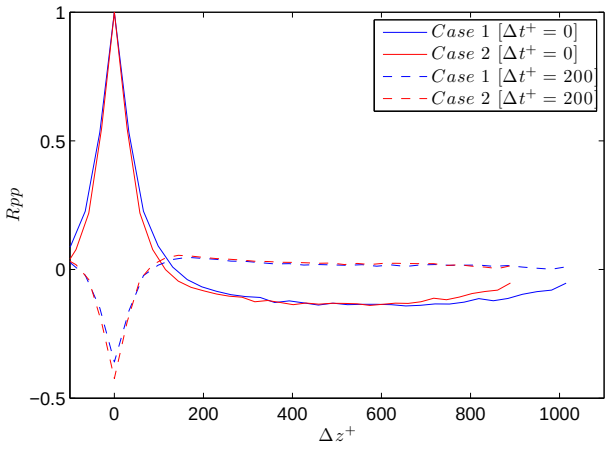

Figure 7. The spanwise distributions of the autocorrelation of the wall pressure fluctuation.

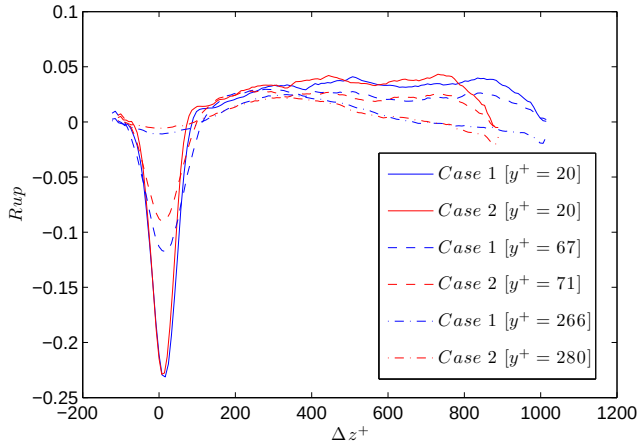

Figure 8. The spanwise distributions of the cross-correlation between the streamwise velocity and pressure fluctuations.

so that it is expected that the resonance does not seriously contaminate the correlations at the large temporal separation.

Figure 7 shows the spanwise distribution of autocorrelation of the wall pressure fluctuation. Except small deference between the negative peak values, distributions of the correlation coefficient are quit similar. The widths of both negative and positive peaks are about 200 wall units. This width corresponds to the dominant disturbance scale and is twice larger than the standard streak spanwise scale of 100 wall units. As reasons of this disagreement, poor spanwise resolution of the pressure sensor array and/or influence of the larger scale disturbance are enumerated. It is considered that the wide plateaus of the positive and negative correlation over $\Delta z^+ = 200$ are from the large scale disturbance that locates higher position than the region the streaks are dominants.

Figure 8 shows the spanwise distribution of correlation

between the streamwise velocity and the wall pressure fluctuations at $\Delta t^+ = 0$, where y^+ is a hot-wire hight in the wall unit. The spanwise traversing step of the hot wire is 0.2 mm. This fine step enables high spanwise resolution of these distributions, though the resolution limit was determined by the hot wire sensor length and the pressure hole diameter that are both 0.5 mm. Comparing the two cases, the distributions are also in good agreement except the negative peak values. The center correlation decreases with the sensor hight from the wall so that these deviations seems to be due to little deference of the hot wire hight in the comparisons. The distributions with the sharp negative peaks and the wide positive plateaus are very similar to that in the autocorrelation of the pressure fluctuation $\Delta t^+ = 0$, except their signs.

Figure 9 shows space-time cross-correlation maps between the streamwise velocity and the wall pressure fluctuations in the buffer layer. The temporal separation was defined as $\Delta t = t_u - t_p$, where t_u and t_p are the measurement time for the velocity and the pressure, respectively. The cross-correlation maps are also very similar. There are not high correlation further than $\Delta t^+ = 5000$. Narrow positive and negative regions around $\Delta z^+ = 0$ noticeably elongate in the temporal direction, suggesting the longitudinal structure of disturbances of small spanwise scale near the wall. Positive and negative regions next to the elongated regions have much wider in the spanwise direction and shorter in time. These indicate that other type of disturbance exists even near the wall.

Figure 10 shows the cross-correlation maps in the log-law region. The cross-correlation maps are still resemble very much. In comparison with the buffer distributions, the positive and negative regions around $\Delta z^+ = 0$ shrink in the temporal direction, keeping the spanwise scale. The longitudinal disturbances of narrow spanwise scale seems to affect the correlation even at this hight. The side correlational regions are also shorten in time and the correlation becomes weaken. From this decrease it is inferred that the wide disturbance is attenuated at least in terms of the intensity of the velocity fluctuation, or that the further distance from the wall on where the pressure fluctuation is measured merely reduced the correlation.

The cross-correlation maps in the outer layer shown in Figure 11 become more complicated. On $\Delta z^+ = 0$, new positive and negative regions appear between the peaks observed in the buffer layer and the log-law region. The negative region in the positive Δt^+ shrinks more and widens in the spanwise direction. The long positive region in $\Delta t^+ < -3000$ still distributes very further in the temporal separation. There exist several positive negative peaks that are not lined in the same Δt^+, suggesting mixture of several dominant disturbances. In the outer layer, no significant deference of the cross-correlation maps between the cases is evident.

Even with the 14 % deference of the free stream velocity, the all statistics obtained here indicate no significant change after the wall unit normalization. In opposition to the authors expectation the tripping manner never affect the boundary layer properties within the present investigation. The tripping device was not changed drastically so that it is necessary to scrutinize turbulent statistics of variety with radical alternation of the trip that converts the transition process. It is still suspended to conclude existence of universality of the zero-pressure-gradient turbulent boundary layer.

The cross-correlation distribution in y^+, Δz^+ and Δt^+ is very invariable with alteration of the tripping manner though they have complicated and continuous positive and negative regions. It is expected that further analysis of this distribution would provide valuable information of the turbulent boundary layer.

CONCLUSION

Influence of a tripping manner on the zero-pressure-gradient turbulent boundary layer are investigation with the two sets of tripping devices. The turbulent statistics of the cross-correlation between the streamwise velocity and the wall pressure fluctuations are not affected by the alteration of the tripping devices. On the other hand, the spatiotemporal cross-correlation map indicates the invariable distribution even they are very complicated. This suggested that the cross-correlation can be utilized for detecting structure of disturbance in turbulent flows.

REFERENCES

P. Schlatter and R. Örlü, 2010, Assessment of DNS data for turbulent boundary layers, NORDITA and Linné FLOW Centre Workshop on Turbulent Boundary Layers.

Kapil A. Chauhan, Peter A. Monkewitz and Hassan M. Nagib, 2009, Criteria for Assessing Experiments in Zero Pressure Gradient Boundary Layers, Fluid Dynamics Research, Vol. 41, Number 2, 021404.

Jens M. Österlund, 1999, Experimental studies of zero pressure-gradient turbulent boundary layer flow, Ph. D. Thesis Royal Institute of Technology Department of Mechanics. Data base http://www.mech.kth.se/ jens/zpg/.

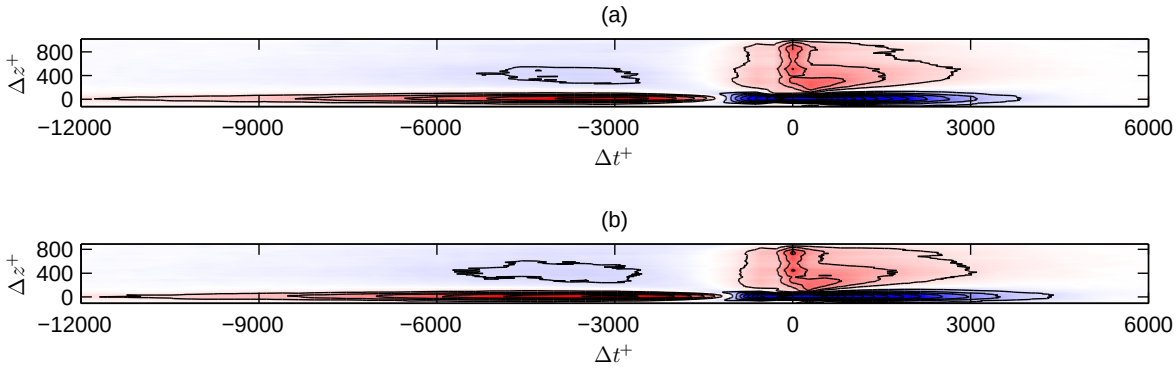

Figure 9. Cross-correlation maps of the streamwise velocity and the wall pressure at $y^+ = 20$. Contour spacing is 1 % and positive and negative regions are colored in red and blue, respectively. (a) Case 1, (b) Case 2.

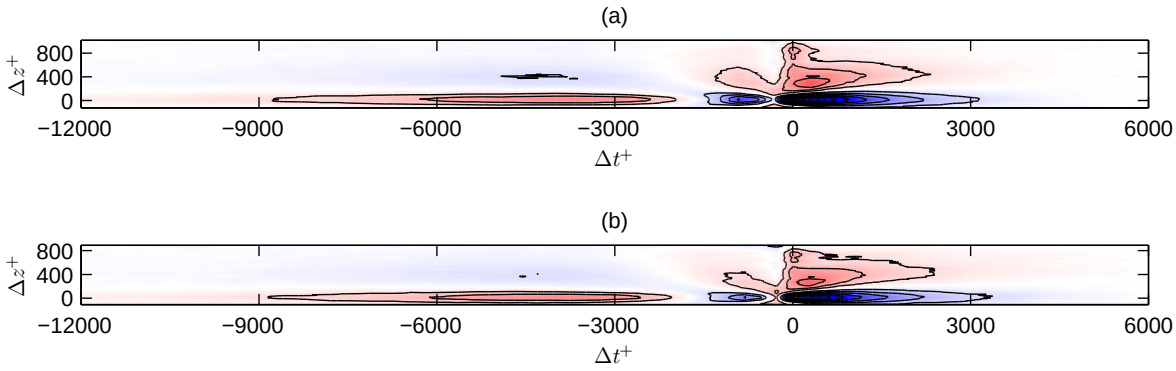

Figure 10. Cross-correlation maps of the streamwise velocity and the wall pressure in the log-law region. Contour spacing and colorizing are same in. Figure 9. (a) Case 1 at $y^+ = 67$, (b) Case 2 at $y^+ = 71$.

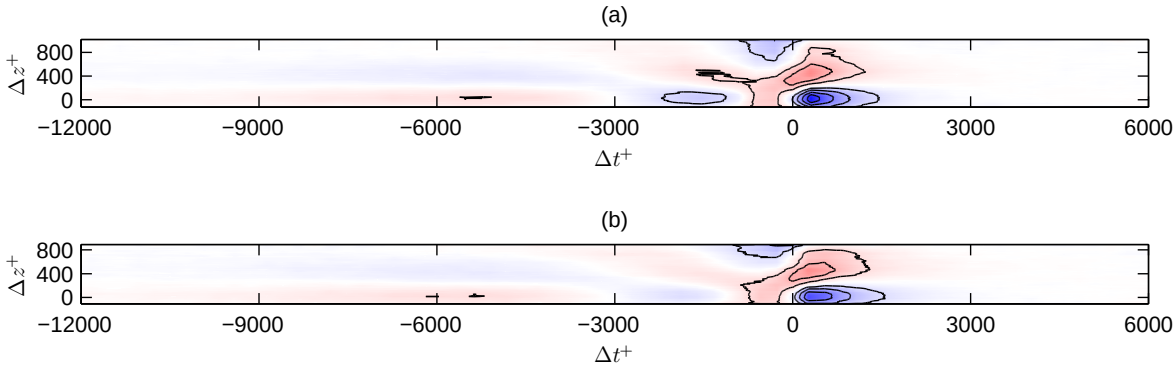

Figure 11. Cross-correlation maps of the streamwise velocity and the wall pressure in the outer region. Contour spacing and colorizing are same in. Figure 9. (a) Case 1 at $y^+ = 266$, (b) Case 2 at $y^+ = 280$.